Available online at www.sciencedirect.com
SCIENCE DIRECT
Polymer 47 (2006) 1970–1978
polymer
www.elsevier.com/locate/polymer

Synthesis, morphology and photophysics of novel hybrid organic–inorganic polyhedral oligomeric silsesquioxane-tethered poly(fluorenyleneethynylene)s

Kan-Yi Pu, Bing Zhang, Zhun Ma, Pei Wang, Xiao-Ying Qi, Run-Feng Chen, Lian-Hui Wang, Qu-Li Fan **, Wei Huang *

Institute of Advanced Materials (IAM), Fudan University, 220 Handan Road, Shanghai 200433, People's Republic of China

Received 5 September 2005; received in revised form 8 December 2005; accepted 9 January 2006

Abstract

A series of novel hybrid organic–inorganic light-emitting materials, polyhedral oligomeric silsesquioxane-tethered poly(fluorenyleneethynylene)s, were successfully synthesized via Sonagashira coupling reaction. The chemical structures of these copolymers were determined by ^{1}H NMR and FT-IR spectra. The morphologies of these copolymers were studied in details using TEM and WAXD. The WAXD data showed that POSS formed aggregation instead of crystallization in the polymer matrix, indicating the significant effect of the backbone constraint on POSS crystallization. Furthermore, it also revealed that the interchain interaction weakened and the interchain distance increased after introducing POSS groups. The TEM data indicated that POSS aggregates were well dispersed in polymer matrix. In accordance with the morphological investigation, the results of UV–vis absorption and photoluminescence emission spectra of these copolymers showed that the tendency toward planar conformation of conjugated backbones reduced to a certain extent due to weakened interchain interaction. Accordingly, these copolymers exhibited the enhanced quantum yields in the solid state. In addition, owing to the thermal and oxygen stability of hybrid POSS, the thermal spectral stability of these polymers was also improved greatly.

Keywords: POSS; Poly(fluorenyleneethynylene)s; Morphology

1. Introduction

Conjugated polymers are under extensive studies for their potential application in organic electronic devices, such as light-emitting diodes (OLEDs) [1], lasers [2], field-effect transistors (FETs) [3], photovoltaic cells [4], and sensors [5]. The performance of organic devices is strongly influenced by the supramolecular organizations or morphologies of the conjugated polymers [6]. In order to fabricate highly efficient OLED, it requires the conjugated materials with minimal chain overlap in the solid state which will result in the less possible formation of low energy sites, including excimers, exciplexs, electrical aggregates and even coplanar conformers [6]. For this purpose, conjugated polymers with bulky groups as side chains, especially dendronized [7] and grafted [8] conjugated polymers, which can be treated as isolated single polymer chains in the solid state were synthesized, and the robust devices using these materials were successfully fabricated. More importantly, these polymers displayed interesting optoelectronic and morphological properties [7a,8a]. Although these materials are current interest for both application and fundamental investigation in the area of organic semiconductors, the critical problem is that they are hard to be prepared due to the long synthetic routes. Thus, conjugated materials which can be easily synthesized but contain the optoelectronic properties comparable to dendronized or grafted conjugated polymers are highly desirable.

Polyhedral oligomeric silsesquioxanes (POSS) consisting of a silica cage surrounded by tunable organic substitution groups are hybrid organic–inorganic nanobuilding blocks [9]. The diameters of POSS range between 1 and 3 nm, depending on the number of silicon atoms and the peripheral substitution groups [9]. In the past several years, POSS have been grafted or copolymerized in a variety of polymeric materials including styrenics [10], acrylics [11], epoxies [12], polyolefins [13], polyimides [14], and others. Interestingly, POSS can

* Corresponding authors. Tel.: +86 21 5566 4188; fax: +86 21 6565 5123.
E-mail addresses: qlfan@fudan.edu.cn (Q.-L. Fan), wei-huang@fudan.edu.cn (W. Huang).

0032-3861/$ - see front matter © 2006 Elsevier Ltd. All rights reserved.
doi:10.1016/j.polymer.2006.01.006

self-assemble into crystals or aggregates in the polymer matrix in which POSS units are incorporated as substituent side units, and POSS crystals or aggregates have an important effect on the properties [13,15]. The extent of possible POSS crystallization or aggregation is attributed to factors such as the nature of the organic periphery of POSS, the mole fraction of POSS, and the interaction of the host chain [13d]. Coughlin et al. has demonstrated that the extent of POSS crystallization can be controlled by the processing condition, which indicated that the POSS morphology in the polymer matrix in which POSS units are incorporated as pendant groups is mainly dependent on the competition of the POSS intermolecular interaction to form POSS crystallization and the polymer backbone constraint to limit POSS crystallization [13c,d].

Due to the bulky volume and more importantly the self-assembly of POSS in polymer matrix, introducing POSS into conjugated polymers as side chains could be a novel effective way to construct conjugated materials with optoelectronic properties comparable to dendronized or grafted conjugated polymers. In fact, most recently, POSS have been introduced into light-emitting materials and were used as star core [16,17], end [18], and pendant components [19–21] to construct new luminescent hybrid materials. The results showed that the presence of bulky POSS in light-emitting materials enhanced the thermal stability and also prevented the formation of electrical aggregates leading to not only high quantum yield but also durable pure light emission. However, the morphologies of the organic–inorganic hybrid conjugated polymers, which are the essential factors to determine their properties, were little investigated. As mentioned previously, POSS self-assembly in polymer matrix will lead to interesting morphology, which is concerned with the material properties. Thus investigating the morphologies of the POSS-containing conjugated hybrid materials is extremely anticipated.

Herein we report the successful synthesis and study of a series of POSS-tethered poly(fluorenyleneethynylene)s (PFEs). PFEs which belong to the family of poly(aryleneethynylene)s (PAEs) are suitable to investigate interplay of morphology and optoelectronic property because of their special conformation-dependent photophysics resulting from the rotation of alkyne-ary single bonds along the backbone [22]. Therefore, we introduced POSS into PFEs and hoped this system could appear obvious optoelectronic property variation on the morphology change of the POSS-tethered PFE hybrids. Their morphologies and optoelectronic properties were investigated. The results indicate that these materials offer promising opportunities both in optoelectronic applications and for fundamental investigation.

2. Experiment section

2.1. Materials and synthesis

2,7-Dibromo-9,9′-dioctylfluorene and 2,7-diethynyl-9,9′-dioctylfluorene were synthesized according to the literature procedures [23]. THF was distilled under nitrogen from sodium benzophenone ketyl. Toluene was purified by distillation from sodium. Other solvents were used without any further purification. Chlorobenzylethylcyclopentyl-POSS (Cl-POSS) and all other reagents were purchased from Aldrich Chemical Co. unless otherwise stated.

2.1.1. 2,7-Dibromo-9,9′-bis(4-hydroxyphenyl)fluorene (*2*)

A mixture of 2,7-dibromofluorenone (9.2 g, 0.027 mol), phenol (17.0 g, 0.18 mol) and methanesulfonic acid (7.8 g, 0.08 mol) in tetrachloromethane (40 g) was stirred at 80 °C for 40 h. The mixture was allowed to cool to room temperature, after which the product was filtered and washed with dichloromethane. Yield 10.0 g (72%) of white powder. ^{1}H NMR (DMSO-d_6), δ (ppm): 9.40 (d, 2H, J=8.1 Hz), 7.88 (d, 2H, J=8.1 Hz), 7.56 (d, 2H, J=8.1), 7.46 (d, 2H, J=1.5 Hz), 6.85 (d, 4H, J=8.7 Hz), 6.65 (d, 4H, J=8.7 Hz). ^{13}C NMR (DMSO-d_6), δ (ppm): 156.3, 153.9, 137.5, 134.5, 130.6, 128.8, 122.8, 121.1, 115.3, 64.0.

2.1.2. 2,7-Dibromo-9,9′-diPOSSfluorene (*3*)

2,7-Dibromo-9,9′-bis(4-hydroxyphenyl)fluorene (91.8 mg, 0.18 mmol), K_2CO_3 (399 mg, 2.89 mmol) and NaI (108 mg, 0.723 mmol) were mixed in *N*,*N*-dimethylformamide (2.25 mL), and the reaction mixture was heated at 50 °C under a nitrogen atmosphere for 2 h. Cl-POSS (400 mg, 0.379 mmol) was dissolved in dry THF (1.8 mL) and added to the mixture, and heating was continued at 60 °C for 2 h. The solution was diluted with water and extracted with chloroform. The extracted organic layer was washed with water two times and concentrated in a vacuum. The yellowy residue was purified by column chromatography (hexane/chloroform 4:1) to afford **3** as white powder. ^{1}H NMR ($CDCl_3$), δ (ppm): 7.60 (d, 2H), 7.47 (m, 4H), 7.32–7.15 (8H), 7.07 (d, 4H), 6.87 (d, 4H), 4,97 (s, 4H), 2.74–2.70 (m, 4H), 1.74–0.83 (130 H). ^{13}C NMR ($CDCl_3$), δ (ppm): 158.3, 145.6, 142.4, 138.4, 131.2, 129.3, 127.0, 125.3, 122.1, 121.4, 114.5, 110.0, 70.4, 29.9, 29,3, 27.5, 27.2, 22.5, 14.4.

2.1.3. General procedure for the preparation of the polymers

2,7-Dibromo-9,9′-dioctylfluorene and 2,7-dibromo-9,9′-diPOSSfluorene (**3**) (total 0.14 mol), 2,7-diethynyl-9,9′-dioctylfluorene (61.6 mg, 0.14 mmol), $Pd(PPh_3)_4$ (8.12 mg, 0.007 mmol), and CuI (3.92 mg, 0.021 mmol) were added to a mixture of degassed toluene (3.92 mL) and diisopropylamine (1.68 mL). The mixture was vigorously stirred at 70 °C for 48 h under nitrogen, then bromobenzene (47 mg, 0.3 mmol) was added for end-capping the polymer for an additional 2 h. After the mixture was cooled to room temperature, it was subjected to a chloroform and water workup. The combined organic phase was washed with water NH_4OH (50%) twice, water twice, and brine once and dried over Na_2SO_4. The solution was removed in vacuum, and the residue was dissolved in chloroform and reprecipitated in methanol twice.

2.1.3.1. Poly(9,9′-di-2-ethyloctyl-2,7-fluorenyleneethynylene) (PFE). ^{1}H NMR ($CDCl_3$), δ (ppm): 7.69 (d, 2H), 7.56 (dd, 4H), 2.0 (m, 4H), 1.25–0.62 (34H).

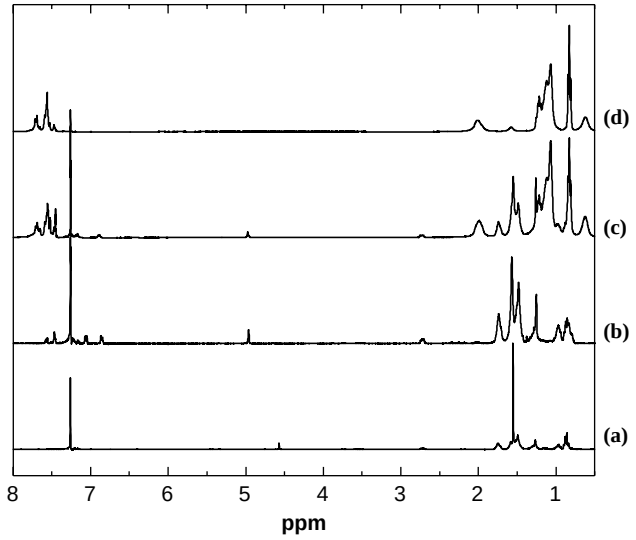

Fig. 1. ^{1}H NMR spectra of (a) Cl-POSS, (b) 3, (c) PFE-POSS-10, and (d) PFE.

2.1.3.2. Poly[9,9′-dioctyfluorene-2,7-yleneethylene-co-diPOSSfluorene-2,7-yleneethylene] (PFE-POSS). The peak positions of ^{1}H NMR spectra of all PFE-POSS copolymers were almost identical. The ^{1}H NMR spectrum of PFE-POSS-10 as an example is demonstrated in Fig. 1.

2.2. Measurements

The NMR spectra were collected on a Varian Mercury Plus 400 spectrometer with tetramethylsilane as the internal standard. FT-IR spectra were recorded on a Shimadzu IRPrestige-21 FTIR-8400s spectrophotometer by dispersing samples in KBr. Thermogravimetric analysis (TGA) was performed on a Shimadzu thermogravimetry and differential thermal analysis DTG-60H at a heating rate of 10 °C/min under N_2. Differential scanning calorimetry (DSC) measurements were performed under a nitrogen atmosphere at heating rates of 20 °C/min, using NETZSCH DSC 200PC apparatus. Gel permeation chromatography (GPC) analysis was conducted with a HP1100 HPLC system equipped with 7911GP-502 and GP NXC columns using polystyrenes as the standard and tetrahydrofuran (THF) as the eluent at a flow rate of 1.0 mL/min and 35 °C. Wide-angle X-ray diffraction (WAXD) data was obtained using Bruker D8 Discover diffractometer with GADDS as a 2D detector. Calibration was conducted using silicon powder and silver behenate. Transmission electron microscopy (TEM) micrographs were obtained using JEOL JEM 2011 electron microscope operation at 200 kV. A drop of polymer chloroform dilute solution was cast onto a carbon-coated copper grid. The samples were dried

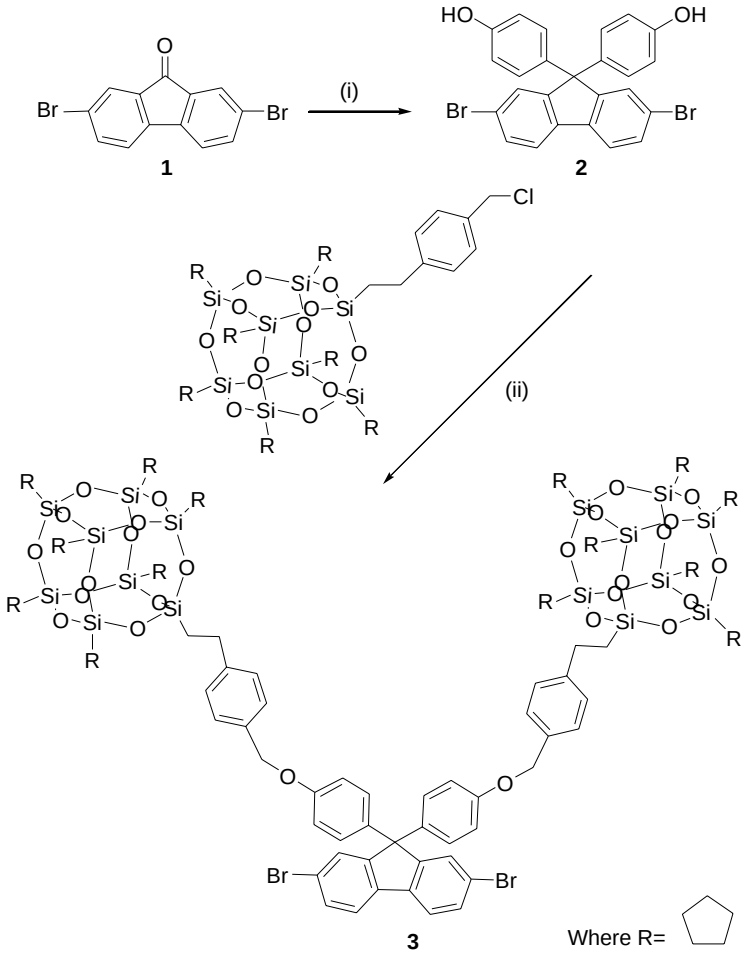

Scheme 1. Synthesis of POSS-substituted fluorene. (i) phenol, methanesulfonic acid, tetrachloromethane, 80 °C. (ii) K_2CO_3, NaI, DMF/THF.

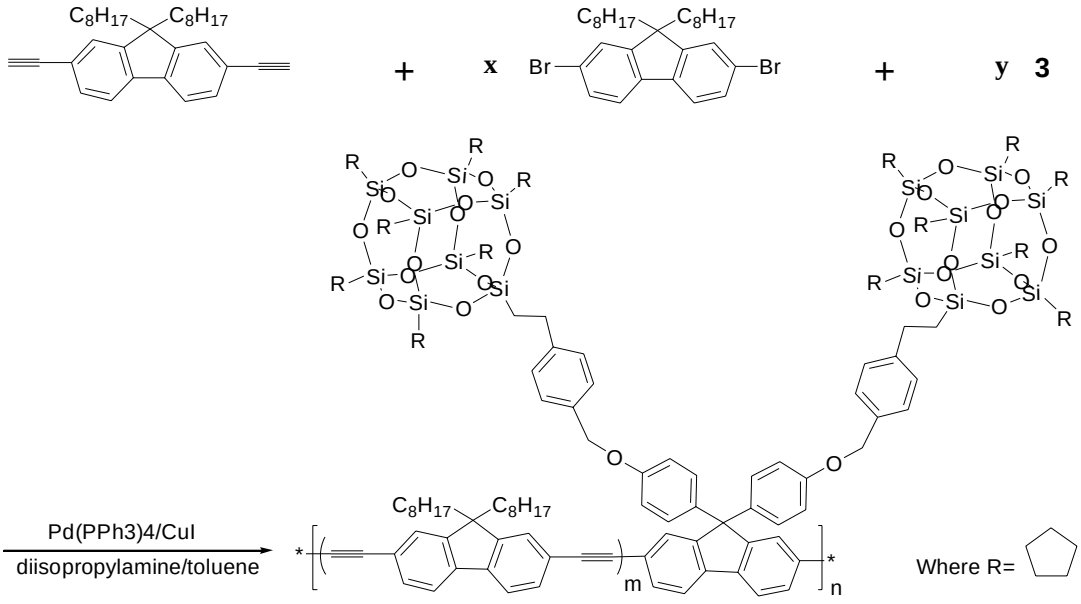

x : y= 100 : 1 **PFE-POSS-1**
x : y = 98 : 2 **PFE-POSS-2**
x : y = 95 : 5 **PFE-POSS-5**
x : y = 90 : 10 **PFE-POSS-10**
x : y = 80 : 20 **PFE-POSS-20**

Scheme 2. Synthesis of PFE-POSS copolymers.

at room temperature prior to measurement. UV–vis spectra were recorded on a Shimadzu 3150 PC spectrophotometer. The concentrations of copolymer solutions were adjusted to about 0.01 mg/mL or less. Fluorescence measurement was carried out on a Shimadzu RF-5301 PC spectrofluorophotometer with a xenon lamp as a light source. Measurement of the absolute PL efficiency was performed on LabsphereIS-080 (8 in.), which contained an integrating sphere coated on the inside with a reflecting material barium sulfate, and the diameter of the integrating sphere was 8 in. PL efficiency was calculated from the software attached by LabsphereIS-080 (8 in.). The polymer films used for measurement of absolute PL efficiency were prepared by spin coating from tetrahydrofuran solution (5 mg/mL) on a quartz plate. The thickness of the films was about 100 nm.

3. Results and discussion

3.1. Synthesis and characterization of the polymers

The synthetic route for POSS-substituted fluorene (**3**) is illustrated in Scheme 1. 2,7-Dibromo-9,9′-bis(4-hydroxyphenyl)fluorene (**2**) is an important intermediate which has been used to introduce other special groups to fluorene monomer, such as dendrons to enhance the steric hindrance and sulphonyl to realize water solubility [7b,24]. In our work, it was coupled with Cl-POSS via Williamson ether reaction to afford compound **3**. PFE-POSS copolymers were synthesized through Sonagashira coupling reaction (Scheme 2). The chemical structures of **3** and copolymers were determined by ^{1}H NMR and FT-IR spectra. Fig. 1 represents the ^{1}H NMR spectra of Cl-POSS, **3**, PFE and PFE-POSS-10. The peak for the benzyl protons of Cl-POSS downshifted from 4.57 to 4.96 ppm in **3**, showing that Cl-POSS had reacted with **2**. The appearance of this peak at 4.96 ppm in the ^{1}H NMR spectra of PFE-POSS copolymers indicated that **3** went on well in Sonagashira coupling reaction. The existence of POSS in **3** and copolymers was confirmed by FT-IR spectra. As shown in Fig. 2, the FTIR spectra of Cl-POSS and **3** displayed a major characteristic peak around 1100 cm^{-1} due to Si–O–Si stretching. For PFE-POSS copolymers, this peak became more and more intensified with the increase of POSS ratio

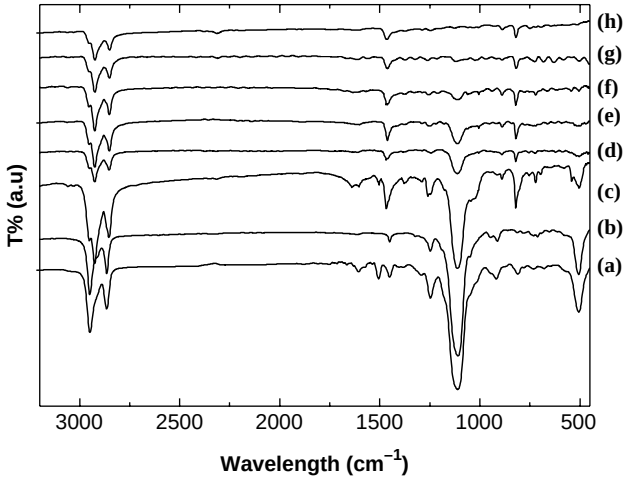

Fig. 2. FT-IR spectra of(a) 3, (b) Cl-POSS, (c) PFE-POSS-20, (d) PFE-POSS-10, (e) PFE-POSS-5, (f) PFE-POSS-2, (g) PFE-POSS-1, (h) PFE.

Table 1
Physical properties of the polymers

Entry	Feed	Actual	M_w (g/mol)	M_n (g/mol)	PDI	Yield (wt%)	T_d (°C)
	POSS (mol%)	POSS (mol%)					
PFE	0	0.0	22000	39000	1.78	73	413
PFE-POSS-1	1	0.8	11000	18000	1.64	58	409
PFE-POSS-2	2	2.0	11000	18000	1.64	59	406
PFE-POSS-5	5	3.2	11000	19000	1.73	54	392
PFE-POSS-10	10	9.2	13000	24000	1.85	52	387
PFE-POSS-20	20	14.2	12000	25000	2.08	55	382

M_n, M_w, and PDI of the polymers were determined by GPC using polystyrene standards.

(Fig. 2). These data further confirmed that the cage structure of POSS did not change in both Williamson ether reaction and Sonagashira coupling reaction, indicating the successful synthesis of PFE-POSS copolymers.

All PFE-POSS copolymers were readily soluble in common organic solvents such as chloroform and THF. Gel permeation chromatography (GPC) revealed that the molecular weights of PFE-POSS copolymers were much lower compared to PFE homopolymer (Table 1), which could be attributed to the steric hindrance caused by POSS during the polymerization process [10e,20]. The actual POSS mole fractions in POSS-PFE copolymers were estimated from ^{1}H NMR according to the ratio between the integrals of peak for the benzyl protons at 4.98 ppm and the alkyl protons adjacent to nine position of fluorene at 2.0 ppm. The results were summarized in Table 1. Glass transfer temperature of PFE was around 56 °C which was in accordance with the literature [25]. We did not observe obvious glass transfer temperature of PFE-POSS copolymers, which indicated that the backbone mobility of the copolymer was strongly retarded by POSS [9b,20]. The decreased T_d of PFE-POSS copolymers with the increased POSS unit could be explained by the weakened interchain interaction owning to the high content of bulky POSS. This phenomenon is analogous to the literature [19], and the decreased interchain interaction was further evidenced by the morphological investigation using WAXD and TEM.

3.2. Morphology

3.2.1. WAXD

Wide-angle X-ray diffraction was used to examine these PFE-POSS samples for POSS aggregates. The diffraction profiles of PFE-POSS copolymers, Cl-POSS and PFE are shown in Fig. 3. Much work has shown that POSS nanoparticles form hexagonal crystal structures [26]. In our work, the spectrum of the pure Cl-POSS showed strong reflections at $2\theta = 8.2$, 11.0, and 18.8° corresponding to d spacing of 10.8, 8.03, and 4.71 Å, respectively, which was a typical WAXD 'fingerprint' of POSS crystals [15]. The spectrum of PFE showed two peaks, a diffuse amorphous halo at 19.6° 2θ with a d spacing of 4.5 Å and a board peak at 5.54° 2θ with a d spacing of 15.9 Å resulting from the packing of the alkyl side chains [27,28]. Hence, it indicated that there was only minor ordering in PFE [29]. The spectra of PFE-POSS copolymers did not exhibit typical features that were characteristic of the structure of the pure Cl-POSS, but they changed dramatically with the increase of mole fraction of POSS. The peak at 5.54° became inconspicuous and finally disappeared, indicating the diminishing of the ordering of the alkyl side chains [28]. Second, a new broad peak at 7.95° with a d spacing of 11.11 Å increased gradually due to the formation of POSS aggregates in the copolymers. The estimated size dimensions (L) of POSS aggregates in PFE-POSS copolymers, based on the half-widths of reflections (β) at 10.5 Å using Debye-Scherrer's equation ($L = 0.89\lambda/(\beta \cos \theta)$), showed a gradual increase in the size of POSS aggregates with the mole fraction of POSS. The apparent size dimensions (L) of POSS aggregates in PFE-POSS-20 and PFE-POSS-10 were 24 and 20 Å, respectively. This method was used to estimate the apparent size dimensions (L) of POSS aggregates by Coughlin et al. firstly [13c–e]. All of these results showed that the Cl-POSS nanoparticles did not form crystallization in PFE-POSS copolymers even though the actual mole fraction of POSS was as high as 14.2% (PFE-POSS-20); meanwhile the disappearance of the peak at 5.54° indicated that the distance between the

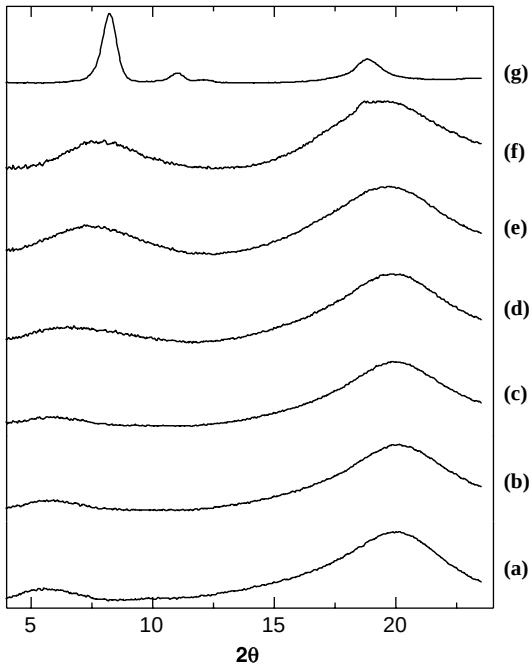

Fig. 3. WAXD profiles of (a) PFE, (b) PFE-POSS-1 (c) PFE-POSS-2, (d) PFE-POSS-5, (c) PFE-POSS-10, (f) PFE-POSS-20, (g) Cl-POSS.

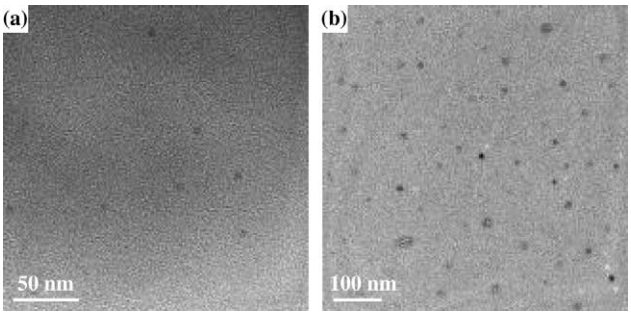

Fig. 4. Transmission electron micrographs of (a) PFE-POSS-5 and (b) PFE-POSS-10.

chains in this copolymers increased and the interchain interaction weakened thanks to the introduction of POSS.

So far, a body of work shows that POSS has strong tendency to crystallize in polymer matrix at relative high mole fraction [13,15], especially the cyclopentyl-substituted POSS (Cp-POSS) [13a]. As shown in Scheme 1, Cl-POSS belongs to the class of Cp-POSS. The exceptive phenomenon of the formation of POSS aggregates instead of POSS crystals in PFE-POSS copolymers is analogous to poly(norbornyl-POSS) copolymers [13a], dicyclopentadiene and norbornenyethyl-POSS crosslinked copolymers [30], and polyimide-side-chain-tethered POSS nanocomposites [14c], which have strong interchain interactions or crosslinked networks that constrain POSS to crystallize. Coughlin and his colleagues also demonstrated that the nature of the backbones of the copolymers in which POSS units are incorporated as pendant groups has a significant effect on POSS crystallization [13c–e]. Cl-POSS did not crystallize in PFE-POSS copolymers, but interestingly it crystallized in the POSS-tethered polyfluorenes which are also conjugated materials with rigid-rod backbones [20]. This phenomenon can be affirmatively attributed to the different natures of the backbones. As reported previously, PFEs which belong to the class of PAEs have an outstanding interchain packing ability in the solid state [22,27]. This ability could be considered as the backbone constraint, which limited POSS to adopt favorable conformations for crystallization in PFE-POSS copolymers. Simultaneously, it was also weakened by the 'anchoring' effect [9b] of POSS judged from the disappearance of the peak at 5.54°.

3.2.2. TEM

The WAXD data indicates that POSS did not crystallize in PFE-POSS copolymers due to the strong backbone constraint, and the size of small POSS aggregates in the polymer matrix were estimated by Debye–Scherrer's equation. However, the real size of POSS aggregates and the distribution of POSS aggregates in the polymer matrix were not definitely confirmed. For this purpose, TEM studies were carried out. The POSS domains show a darker image compared with PFE-POSS backbones, allowing not using a staining agent [13e]. Fig. 4 showed the TEM micrographs of PFE-POSS-5 and PFE-POSS-10 which were obtained after the confirmation of the chemical compositions using energy dispersive X-ray analysis. The size of POSS aggregates in PFE-POSS-5 was slightly smaller than that in PFE-POSS-10 (Fig. 4), which was consistent with the result of the WAXD analysis that the size of POSS aggregates gradually increased with the increase of the mole fraction of POSS. But the value of POSS aggregates size (6–15 nm) obtained from TEM was larger than that (2–2.4 nm) obtained from the WXAD, which could be explained by the fact that when the intensity of the reflection is low, using Debye–Scherrer's equation to estimate the POSS aggregate size will result in a larger error [31]. Regardless, TEM micrographs displayed that POSS aggregates were well dispersed in PFE-POSS copolymers.

3.3. Photophysics

Due to the relatively free rotation of alkyne-ary single bonds along the backbone of PAEs, it is known that this class of conjugated polymers has a conformation-dependent photophysics [22,32]. Recently, Bunz et al. have reinvestigated photophysics of poly[*p*-(2,5-didodecylphenylene)ethynylene] and concluded that the large red-shift (around 50 nm) in the emission spectrum resulted from the planarization of the backbones rather than the formation of electrical aggregates, meanwhile, the absorption spectra did not red shift so much [33]. As shown in Table 2, PFE also showed a large red-shift in emission spectrum, which was in good accordance with the literature reported by Kim et al. Because of the relatively high emission intensity and narrower emission bandwidth of PFE in the solid state, the possibility that this red-shift resulted from electrical aggregates was naturally ruled out [34]. As

Table 2
Photophysical properties of PFE-POSS copolymers and PFE in the dilute THF solutions and thin films

Entry	$\lambda_{max,abs}$ (nm)[a]		$\lambda_{max,pl}$ (nm)[a]		Quantum yield of thin films
	Solution	Film	Solution	Film	
PFE	390 (409)	395 (417)	422 (445)	476 (506)	0.13
PFE-POSS-1	387 (408)	395 (417)	424 (446)	476 (507)	0.22
PFE-POSS-2	387 (408)	391 (416)	425 (446)	478 (507)	0.24
PFE-POSS-5	387 (410)	391 (415)	426 (452)	478 (507)	0.24
PFE-POSS-10	385 (405)	391 (416)	423 (445)	476 (508)	0.25
PFE-POSS-20	385 (405)	391 (415)	422 (445)	476 (504)	0.27

[a] Data in parentheses are wavelengths of shoulders and subpeaks.

mentioned in the literature [34], it could be attributed to the formation of a small portion of planar segments with extended effective conjugation in the solid state. It was worth to note that this small portion of segments with planar conformations could act as energy accepters, while the other segments could act as energy donors. Therefore, compared with the spectra of the dilute solutions, because the amount of planar segments was very small, the maximal peaks in UV–vis spectra of the thin films did not change significantly, which mainly exhibited the absorption of the segments with the close conformations to that in dilute solution; whereas, due to the highly efficient energy transfer from the numerous twisted segments to the few planar segments in the thin films, the maximal peak in emission spectra was located at 475 nm, which resulted in this 50 nm red-shift and in turn a large Stokes shift. This phenomenon was appreciably similar with the energy transfer process of poly(fluorene-*co*-thiophene) self-forming donor–accepter systems [35].

As below, we studied the effect of POSS on the photophysical properties of PFE system. Similarly, PFE-POSS copolymers also showed the red-shift. Fig. 5 demonstrates UV–vis absorption spectrum and photoluminescence emission spectrum of PFE in the dilute THF solution. UV–vis absorption spectra and photoluminescence emission spectra of PFE-POSS copolymers were equal to that of PFE. Fig. 6 shows UV–vis absorption spectra and photoluminescence emission spectra of PFE and PFE-POSS copolymers in the thin films. Comparing the emission spectra in the dilute THF solutions with these in the thin films, we can see that the large red shift (about 50 nm) still occurred for PFE-POSS copolymers just like PFE (the detailed data about the spectra were summarized in Table 2). The existence of the large red-shift of PFE-POSS copolymers showed that although introducing bulky POSS into PFE as pendant groups reduced the interchain interaction, the small portion of planar segments which were the energy acceptors here still existed in these copolymers. However, we found that in the solid state, there were visible differences between the spectra of PFE-POSS copolymers and that of PFE. In the UV–vis absorption spectra which were normalized according to the peak around 391 nm (Fig. 6), the intensity of

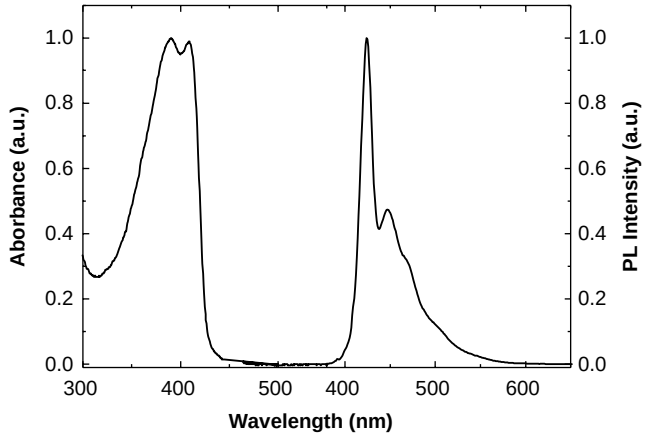

Fig. 5. UV–vis absorption spectrum and photoluminescence emission spectrum of PFE in the dilute THF solution.

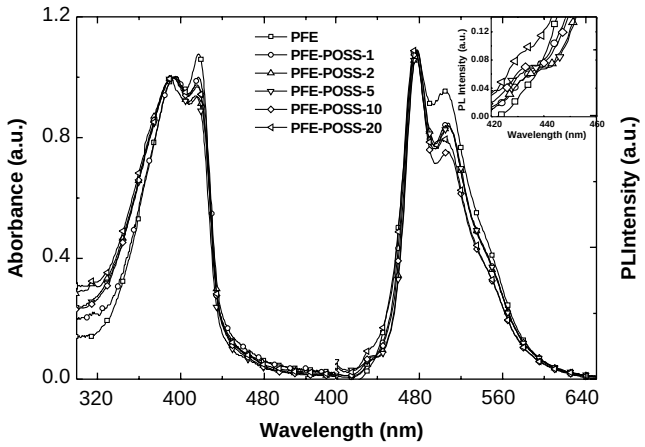

Fig. 6. UV–vis absorption spectra and photoluminescence emission spectra of these polymers in the thin films, which were normalized according to the absorption peak around 391 nm and the maximal emission peak around 476 nm, respectively. Inset: Enlarged photoluminescence emission spectra of these polymers in the thin films from 420 to 460 nm.

the absorption peak at longer wavelength around 416 nm for PFE-POSS copolymers were weaker than PFE, and more importantly, in the emission spectra which were normalized according to the maximal emission peak around 476 nm, as shown in the inset of Fig. 6, the peak around 425 nm which was the maximal emission peak in solution concerning the twisted segments remained for PFE-POSS copolymers, while it was invisible for PFE due to the efficient energy transfer from the twisted segments to the planar segments in the solid state. Comparing with this highly efficient energy transfer in PFE, such a residue of the peak around 425 nm in emission spectra of PFE-POSS copolymers indicated the relatively incomplete energy transfer from the twisted segments to the planar segments in PFE-POSS copolymers. It could be attributed to the fact that the interchain distance which was related to the energy transfer distance increased due to the existence of POSS as bulky side chains, and also to the possibility that the tendency towards planar conformation in the solid state was reduced to a certain extent as result of weakened interchain interaction.

As reported previously, the introduction of bulky POSS increased the quantum yield and the thermal spectra stability of the conjugated polymers [19–21]. The quantum yields of PFE-POSS copolymers in the thin films increased gradually with the mole fraction of POSS because of the reduced interchain interaction (Table 2) [19–21]. In order to investigate the thermal spectra stability of PFE-POSS copolymers in air, the emission spectra of the annealed films in respect to the fresh films are showed in Fig. 7. As we known, PAEs are not stable in air at elevated temperature due to the occurrence of curing reaction of the triple bonds [36]. Thus, after annealing in air, the emission spectrum of PFE film changed to be featureless with a significant decrease in the relative intensity, which was similar to the literature [36]. And the quantum efficiency was decreased to 0.03. In accordance with the literatures [19–21], when introducing bulky POSS into the polymer as pendant groups, because of the outstanding inorganic thermal and

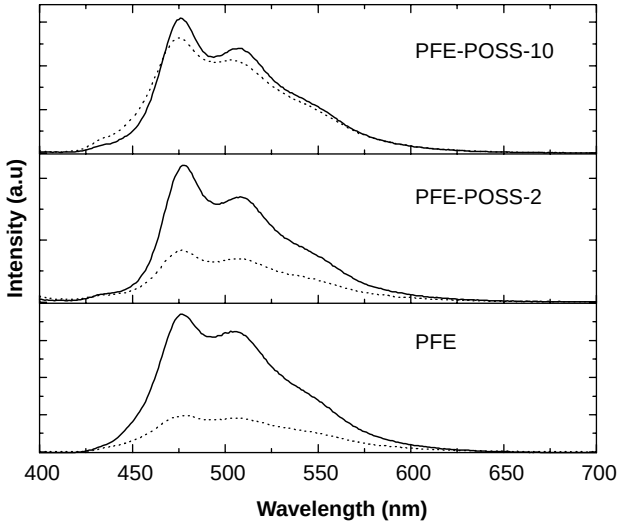

Fig. 7. Photoluminescence emission spectra of (a) PFE, (b) PFE-POSS-2, and (c) PFE-POSS-10 films before (solid line) and after (dash line) annealing at 150 °C for 1 h in air.

oxygen stability of hybrid POSS, the thermal spectra stability improved gradually and clearly with the increase of the mole fraction of POSS (Fig. 7). As a result, the quantum efficiency of the thermal treated PFE-POSS-10 film was almost identical to that before the thermal treatment.

4. Conclusion

In summary, we have successfully synthesized a series of novel hybrid organic–inorganic conjugated polymers, PFE-POSS copolymers, via Sonagashira coupling reaction. The solid state morphologies of these copolymers have been studied in details using WAXD and TEM. POSS formed small aggregates instead of crystals in the polymer matrix because of the strong interchain interaction of the backbones, which demonstrated that the backbone constraint played an important role in the final POSS morphology in the polymer matrix. Furthermore, these POSS aggregates were well dispersed in the polymer matrix. On the other side, the interchain packing ability and the tendency towards planar conformation of the conjugated polymers were reduced owing to the presence of POSS as side chains. PFE-POSS copolymers exhibited enhancement of quantum yields and the improvement of thermal spectral stability in the solid state compared to PFE. All these results showed that besides dendronization and graftation of conjugated polymers, introducing POSS into conjugated materials as pendant groups is another effective way to construct outstanding conjugated materials not only for the application of OLEDs but also for fundamental investigation such as interplay of morphology and optoelectronic property.

Acknowledgements

This work was financially supported by the National Natural Science Foundation of China under Grants 60325412, 90406021, 20504007 and 50428303 as well as the Shanghai Commission of Science and Technology under Grants 03DZ11016 and 04XD14002 and the Shanghai Commission of Education under Grant 2003SG03. K. Y. PU thanks the scholarship and top-up provided by Fudan University and IAM.

References

[1] Friend RH, Gymer RW, Holmes AB, Burroughes JH, Marks RN, Taliani C, et al. Nature (London) 1999;397:121.
[2] McGehee MD, Heeger AJ. Adv Mater 2000;12:1655.
[3] Sirringhaus H, Tessler N, Friend RH. Science 1998;280:1741.
[4] Sariciftci NS. Curr Opin Solid State Mater Sci 1999;4:373.
[5] Chen L, McBranch DW, Wang H, Helgeson R, Wudl F, Whitten DG. Proc Natl Acad Sci USA 1999;96:12287.
[6] Schwartz BJ. Annu Rev Phys Chem 2003;54:141.
[7] (a) Setayesh S, Grimsdale AC, Weil T, Enkelmann V, Müllen K, Meghdadi F, et al. J Am Chem Soc 2001;123:946.
(b) Chou C, Shu C. Macromolecules 2002;35:9673.
[8] (a) Breen CA, Deng T, Breiner T, Thomas EL, Swager TM. J Am Chem Soc 2003;125:9942.
(b) Breen CA, Tischler JR, Bulović V, Swager TM. Adv Mater 2005;17:1981.
(c) Breen CA, Rifai S, Bulović V, Swager TM. NanoLett 2005;5:1597.
[9] (a) Baney RH, Itoh M, Sakakibara A, Suzuki T. Chem Rev 1995;95:1409.
(b) Phillips SH, Haddadd TM, Tomczak SJ. Curr Opin Solid State Mater Sci 2004;8:21.
[10] (a) Romo-Uribe A, Mather PT, Haddad TS, Lichtenhan JD. J Polym Sci, Part B: Polym Phys 1998;36:1857.
(b) Xu H, Kuo SW, Lee JS, Chang FC. Polymer 2002;43:5117.
(c) Haddad TS, Viers BD, Phillips SH. J Inorg Organomet Polym 2002;11:155.
(d) Zheng L, Kasi RM, Farris RJ, Coughlin EB. J Polym Sci, Part A: Polym Chem 2002;40:885.
(e) Fu BX, Lee A, Haddad TS. Macromolecules 2004;37:5211.
(f) Lichtenhan JD, Otonari YA, Carr MJ. Macromolecules 1995;28:8435.
[11] (a) Pyun J, Matyiaszewsi K, Wu J, Kim GM, Chun SB, Mather PT. Polymer 2003;44:2739.
(b) Zhang W, Fu BX, Seo Y, Schrag E, Hsiao B, Mather PT, et al. Macromolecules 2002;35:8029.
(c) Kopesky ET, Haddad TS, Cohen RE, McKinley GH. Macromolecules 2004;37:8992.
(d) Lee A, Lichtenhan JD. Macromolecules 1998;31:4970.
[12] (a) Lee A, Lichtenhan JD. J Appl Polym Sci 1999;73:1993.
(b) Li GZ, Wang L, Toghiani H, Daulton TL, Koyama K, Pittman CU. Macromolecules 2001;34:8686.
(c) Ni Y, Zheng S, Nie K. Polymer 2004;45:5557.
(d) Strachota A, Kroutilova I, Kovarova J, Matejka L. Macromolecules 2004;37:9457.
(e) Matejka L, Strachota A, Plestil J, Whelan P, Steinhart M, Slouf M. Macromolecules 2004;37:9449.
(f) Tsuchida A, Bolin C, Sernetz FG, Frey H, Muhlhaupt R. Macromolecules 1997;30:2818.
[13] (a) Mather PT, Jeon HG, Romo-Uribe A, Haddad TS, Lichtenhan JD. Macromolecules 1999;32:1194.
(b) Zheng L, Farris RJ, Coughlin EB. Macromolecules 2001;34:8034.
(c) Waddon AJ, Zheng L, Farris RJ, Coughlin EB. NanoLett 2002;2:1149.
(d) Zhang L, Waddon AJ, Farris RJ, Coughlin EB. Macromolecules 2002;35:2375.
(e) Zheng L, Hong S, Cardoen G, Burgaz E, Gido SP, Coughlin EB. Macromolecules 2004;37:8606.

[14] (a) Huang J, He C, Xiao Y, Mya KY, Dai J, Siow YP. Polymer 2003;44:4491.
(b) Tamaki R, Choi J, Laine RM. Chem Mater 2003;15:793.
(c) Leu CM, Chang YT, Wei KH. Macromolecules 2003;36:9122.
[15] Waddon AJ, Coughlin EB. Chem Mater 2003;15:4555.
[16] (a) Tamaki R, Tanaka Y, Asuncion MZ, Choi J, Lame RM. J Am Chem Soc 2001;123:12416.
(b) He C, Xiao Y, Huang J, Lin T, Mya KY, Zhang X. J Am Chem Soc 2004;126:7792.
(c) Brick CM, Ouchi Y, Chujo Y, Lame RM. Macromolecules 2005;38:4661.
(d) Brick CM, Tamaki R, Kim SG, Asuncion MZ, Roll M, Nemoto T, et al. Macromolecules 2005;38:4655.
(e) Sellinger A, Tamaki R, Laine RM, Ueno K, Tanabe H, William E, et al. Chem Commun 2005;3700.
[17] Lin WJ, Chen WC, Wu WC, Niu YH, Jen AKY. Macromolecules 2004;37:2335.
[18] Xiao S, Nguyen M, Gong X, Cao Y, Wu H, Moses D, et al. Adv Funct Mater 2003;13:25.
[19] Lee J, Cho HJ, Jung BJ, Cho NS, Shim HK. Macromolecules 2004;37:8523.
[20] Chou CH, Hsu SL, Dinakaran K, Chiu MY, Wei KH. Macromolecules 2005;38:745.
[21] Takagi K, Kunii S, Yuki Y. J Polym Sci, Part A: Polym Chem 2005;43:2119.
[22] Bunz UHF. Chem Rev 2000;100:1650.
[23] Liu B, Yu W, Pei J, Liu S, Lai Y, Huang W. Macromolecules 2001;34:7932.
[24] Burrows HD, Lobo VMM, Pina J, Ramos ML, Melo JSD, Valente AJM, et al. Macromolecules 2004;37:7425.
[25] Zhan X, Liu Y, Zhu D, Huang W, Gong Q. Chem Mater 2001;13:1540.
[26] (a) Barry AJ, Daudt WH, Domicone JJ, Gilkey JW. J Am Chem Soc 1955;77:4248.
(b) Larsson K. Ark Kemi 1960;16:203.
(c) Larsson K. Ark Kemi 1960;16:209.
(d) Larsson K. Ark Kemi 1960;16:215.
[27] Bunz UHF, Enklemann V, Kloppenburg L, Jones D, Shimizu KD, Claridge JB, et al. Chem Mater 1999;11:1416.
[28] (a) Yasuda T, Imase T, Nakamura Y, Yamamoto T. Macromolecules 2005;38:4687.
(b) Tanto B, Guha S, Martin CM, Scherf U, Winokur MJ. Macromolecules 2004;37:9438.
[29] Chen SH, Su AC, Han SR, Chen SA, Lee YZ. Macromolecules 2004;37:181.
[30] Constable CS, Lesser AJ, Coughlin EB. Macromolecules 2004;37:1276.
[31] Turri S, Levi M. Macromolecules 2005;38:5569.
[32] (a) Levitus M, Schmieder K, Ricks H, Shimizu KD, Bunz UHF, Garibay MAG. J Am Chem Soc 2001;123:4529.
(b) Levitus M, Schmieder K, Ricks H, Shimizu KD, Bunz UHF, Garibay MAG. J Am Chem Soc 2002;124:8181.
(c) Levitus M, Zepeda G, Dang H, Godinez C, Khuong TAV, Schmieder K, et al. J Org Chem 2001;65:3188.
(d) Beeby A, Findlay K, Low PJ, Marder TB. J Am Chem Soc 2002;124:8280.
[33] Bunz UHF, Imhof JM, Bly RK, Bangcuyo CG, Rozanski L, Bout DAV. Macromolecules 2005;38:5892.
[34] (a) Kim DY, Hong JM, Kim JK, Cho HN, Kim CY. Macromol Symp 1999;143:221.
(b) Kim DY. Prog Polym Sci 2000;25:1089.
[35] (a) Vamvounis G, Holdcroft S. Adv Mater 2004;16:716.
(b) Vamvounis G, Schulz GL, Holdcroft S. Macromolecules 2004;37:8897.
[36] Hong JM, Cho HN, Kim DY, Kim CY. Synth Met 1999;102:933.